SUPPORTING INFORMATION

Cooperative Binding Energetics of CytR and CRP Support a Quantitative Model of Differential Activation and Repression of CytR-regulated Class III *Escherichia coli* Promoters

Allison K. Holt and Donald F. Senear

Address:
Department of Molecular Biology and Biochemistry, University of California, Irvine CA 92697.

1. Footprint Titration of Analysis of CRP Binding to *nupGP* and *tsxP2*.

Consistent with previous reports, DNase I footprints of CRP binding to wild type *nupGP* delineate distinct regions that correspond to CRP1 and CRP2 (*1*). Figure S1A presents results when the program ImageQuant was used to obtain the fractional change in DNase I mediated cleavage in contiguous bands (or "blocks") of a representative titration experiment. Analysis using eq. 1 (see *Experimental Procedures*) to obtain the loading free energy changes for CRP binding to each site, $\Delta G_{load,i}$ (*2*) yields $\Delta G_{load,1} -10.8 \pm 0.18$ kcal/mol (CRP1) and $\Delta G_{load,2} -14.3 \pm 0.10$ kcal/mol (CRP2). CRP binds non-cooperatively (*1, 3-7*); consequently, $\Delta G_{load,i}$ is equal to the intrinsic free energy change for CRP binding, which we denote ΔG_i.

Figure S1

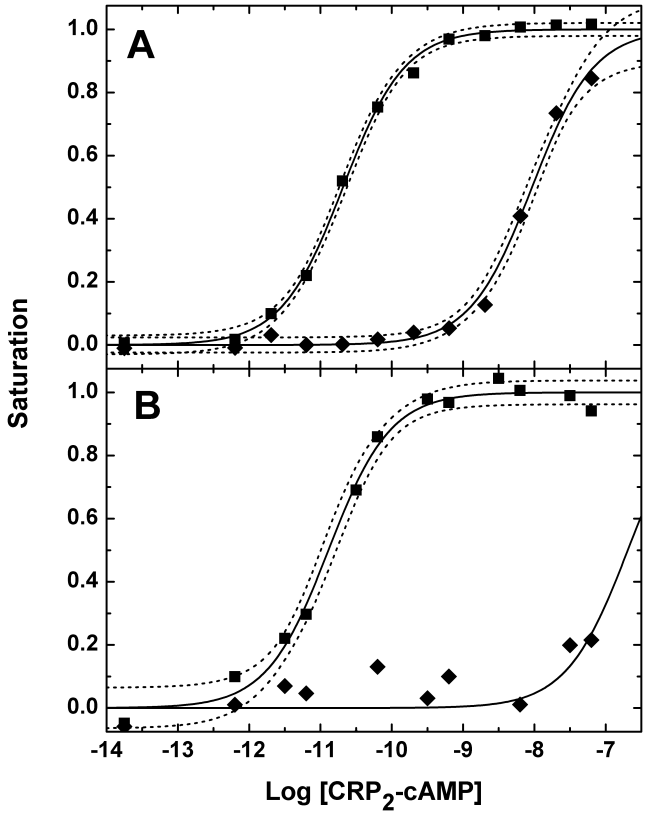

CRP binding to *nupGP*. *A*. wild type promoter. *B*. CRP1⁻ promoter. Fractional saturation of CRP1 (◆) and CRP2 (■) are plotted as a function of the log concentration of the active form of cAMP-liganded CRP dimer. Solid curves represent separate analysis of the protection data for each site according to Equation 1; these yield $\Delta G_2 = -14.3 \pm 0.10$ and -14.6±0.19 kcal/mol for CRP binding to wild type and CRP1⁻ promoters, respectively, and $\Delta G_1 = -10.8 \pm 0.18$ kcal/mol for wild type and ΔG_1=-9 kcal/mol as a lower limit to the affinity for CRP1⁻. Dashed curves are the 65% confidence limits of the fitted curves.

Titration experiments were also conducted on reduced-valence promoters, CRP1⁻ and CRP2⁻. These were generated by introducing base pair substitutions at positions in the CRP sites known

to be critical for sequence-specific recognition and binding as described above (*Experimental Procedures*). Pederson et al (*1*) have reported that CytR binding to *nupGP* CytO displaces CRP1 by two bp downstream, to a site located at 40.5 bp upstream from the transcription start site. A second substitution was made (Figure 1) to eliminate the possibility of CRP-binding in this register.

Figure S1B shows representative results. There is no significant difference between CRP binding to CRP2 of the wild type (Panel A) and CRP1$^-$ (Panel B; $\Delta G_2 = -14.6 \pm 0.19$ kcal/mol) promoters. This indicates that the bp substitutions in CRP1 do not affect CRP2. Site CRP1$^-$ shows only very weak protection and this at only the two highest CRP concentrations where non-specific binding begins to obscure the analysis. These data do not define the maximum protection upper endpoint. Consequently an unconstrained fit does not yield a bounded value of $\Delta G_1'$ (the prime denotes a mutated site). However, if we assume the same maximum protection as observed for CRP2 and fix $P_{\max}$ in eq. 1 at this value, $\Delta G_1' = -9.0$ kcal/mol is obtained. This should be considered the upper limit to the affinity. The bp substitutions have decreased the affinity by at least two orders of magnitude, consistent with previous experience (*3, 5, 6*).

The affinity of CRP for binding to CRP2$^-$ is similarly reduced. However, wild type CRP2 is an unusually high affinity site such that even with a two order of magnitude decrease, CRP2$^-$ retains appreciable affinity, *i.e.*, $\Delta G_2' = -12.4 \pm 0.7$ kcal/mol. It is evident that such high remaining affinity cannot be ignored in developing a statistical thermodynamic model for the interactions between the regulatory proteins at *nupGP*.

Average ΔG_i values are compiled in Table S1. *NupGP* CRP2 is the highest affinity CRP site among the CytR-regulated promoters and CRP1 the lowest. These differ by 200-fold with the

consequence that CRP2 is essentially fully occupied in the absence of CytR prior to any binding to CRP1, a situation not found in any other CytR-regulated promoter.

Table S1: Loading free energy changes ($\Delta G_{load,i}$) for binding of CRP and CytR to *nupGP* [a]

				Operator Site				
NupG valence	Titrant	Effector[b]	No. of expts[c]	CRP2	CytR at CRP2	CytO	CRP1	CytR at CRP1
Wild type, CRP1-, CRP2-	CRP	None	6	-14.5 ± 0.2 (-12.4± 0.7)[d]			-11.4 ± 0.4 (≥-9.0)[d]	
Wild type, CRP1-, CRP2-	CytR	None	7		-9.4 ± 0.4	-10.4 ± 0.3		-9.1 ± 0.3
Wild type	CRP	CytR	3	-14.1 ± 0.4		-	-12.5 ± 0.3	
CRP1-	CRP	CytR	3	-14.2 ± 0.6		-	-11.3 ± 0.2	
CRP2-	CRP	CytR	3	-13.6 ± 0.4		-	-12.6 ± 0.3	
Wild type	CytR	CRP	2	-		-12.7 ± 0.5	-	
CRP1-	CytR	CRP	3	-		-13.1 ± 0.3	-	
CRP2-	CytR	CRP	2	-		-13.2 ± 0.5	-	
Wild type	CRP	CytR, cytidine	2	-14.1 ± 0.4		-	-12.5 ± 0.3	
CRP1-	CRP	CytR, cytidine	2	-14.2 ± 0.4		-	-11.2 ± 0.5	
CRP2-	CRP	CytR, cytidine	2	-12.3 ± 0.1		-	-10.6 ± 0.1	
Wild type	CytR	CRP, cytidine	2	-		-11.3 ± 0.3	-	
CRP1-	CytR	CRP, cytidine	3	-		-12.1 ± 0.2	-	
CRP2-	CytR	CRP, cytidine	2	-		-11.1 ± 0.8	-	

[a] Standard free energy changes for saturation of *nupGP* operators with either CRP$(cAMP)_1$ or CytR in the presence or absence of effector ligands are as indicated. Values of $\Delta G_{load,i}$ (in kcal/mol ± the 65% confidence interval) were obtained by separate analysis of individual site binding curves as described in the text.

[b] Effector concentrations: CRP, 0.1 μM (total dimer); cAMP, 150 μM; CytR, 0.1 μM (dimer); cytidine, 2 mM.

[c] Values are means of multiple determinations (± s.d.). The number of separate experiments represented in the means reported is indicated.

[d] Values for CRP1 of CRP1- promoter and for CRP2 of CRP2- promoter.

Figure S2 presents representative titration data for CRP binding to wild type *tsxP2*. Panel A presents the analysis of blocks according to the usual approach as outlined in the *Experimental*

Procedures. CRP binding is typically characterized both by bands that are protected and by others that become hypersensitive to DNase I. The latter make a negative contribution to the fractional protection. In this case, the combination of opposite effects results in a relatively modest change in net protection (Figure 3A). Despite this, these data do provide a relatively precise estimate of $\Delta G_1 = -11.9 \pm 0.17$ kcal/mol.

Figure S2

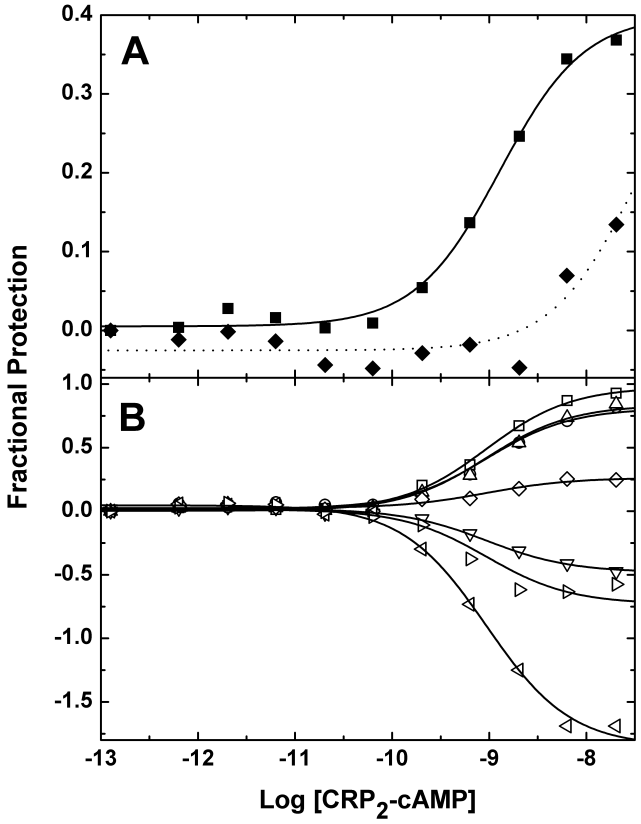

CRP binding to the wild type *tsxP2*. *A*. Fractional protection of CRP1 (■) and CRP2 (◆) from analysis of blocks of bands. Curves represent separate analysis of each site according to Equation 1. The dashed line used for CRP2 denotes the constraint used in the fitting as discussed in the text. This yields $\Delta G_1 = -11.9 \pm 0.17$ and $\Delta G_2 = -10.0 \pm 0.3$ kcal/mol. *B*. Analysis of CRP1 by individual bands. All seven distinct bands included in the block analyzed in *A*. are shown, of which four show protection and three, hypersensitivity. Global analysis of these bands using Equation 1 yields $\Delta G_1 = -12.1 \pm 0.08$.

In consideration of these opposite contributions we also selected seven individual bands within the CRP1 block (Figure S2B) that are sufficiently distinct to analyze using the program SAFA (*8*). We anticipated that this alternative approach might improve signal-to-noise. Four of the bands selected are protected with maximum fractional protection ranging from 0.25-1; three others are hypersensitive with increased DNase I cutting ranging from 50-200%. Results of

individual fits of the seven individual bands are indistinguishable from which we conclude that each band, whether protected or hypersensitive, reflects the same molecular interaction, *i.e.*, binding of CRP to CRP1. This result validates the application of this strategy to discriminate between bp positions that respond to either the same, or to different binding events, as used below.

Global analysis of the individual fractional protection of these seven bands yielded $\Delta G_1 = -12.1 \pm 0.08$ kcal/mol, a value that is indistinguishable from the standard block analysis, but whose precision is improved. The average of these two determinations is listed as the value of ΔG_1 in Table S2.

Table S2: Loading free energy changes ($\Delta G_{load,i}$) for binding of CRP and CytR to the *tsxP2* regulatory region[a]

			Operator Site			
Titrant	Effector[b]	No. of expts[c]	CRP2	CytO	CRP1	CytR at CRP1
CRP	None	4	≥-10		-11.8 ± 0.4	
CytR	None	4		-10.4 ± 0.3		-10.4 ± 0.3
CRP	CytR	2	n.d.		-11.2 ± 0.1	
CytR	CRP	2		-11.9 ± 0.2		

[a] Standard free energy changes for saturation of *tsxP2* operators with either CRP(cAMP)$_1$ or CytR alone or in the presence or absence of the other protein as indicated. Values of $\Delta G_{load,i}$ (in kcal/mol ± the 65% confidence interval) were obtained by separate analysis of individual site binding curves as described in the text.

[b] Effector concentrations: CRP, 0.1 μM (total dimer); cAMP, 150 μM; CytR, 0.1 μM (dimer).

[c] Values are means of multiple determinations (± s.d.). The number of separate experiments represented in the means reported is indicated.

In contrast to CRP1, CRP2 shows protection at only the two highest CRP concentrations (Figure S2A). Consequently, analysis requires that P_{max} be fixed in eq. 1 as was done for *nupGP* CRP1$^-$ above. As before, we assumed the same maximum protection for CRP2 as was

obtained for CRP1. This analysis yielded $\Delta G_2 = -10.0 \pm 0.3$ kcal/mol, which should be considered to reflect an upper limit to the intrinsic binding affinity. Thus, we find CRP2 to be at least twenty-five-fold weaker than CRP1. The result is consistent qualitatively with a previous report by Valentin-Hansen and colleagues (*9*) who find the affinity difference to be in the same direction. Their semi-quantitative titrations suggest only about a five-fold difference between the two sites, but also apparent affinities that are more than two orders of magnitude weaker than we find under our conditions.

2. Footprint Titration Analysis of CytR Binding to *nupGP* and *tsxP2*.

CytR binding was analyzed similarly. We have shown previously that CytR binds to variable arrays of CytR recognition motifs in *deoP2*, *cddP* and *udpP* (*3, 5, 6*). In addition to CytO these typically include a second site that overlaps and occludes CRP1 and a third site that overlaps and occludes CRP2. We observe these three distinct sites in *nupGP* (Figure S3) and obtain $\Delta G_3 = -10.8 \pm 0.30$ (CytO), $\Delta G_4 = -9.6 \pm 0.35$ (CRP1 site) and $\Delta G_5 = -9.7 \pm 0.40$ (CRP2 site) kcal/mol, respectively. We also observe a fourth site located proximal to the transcription start

Figure S3

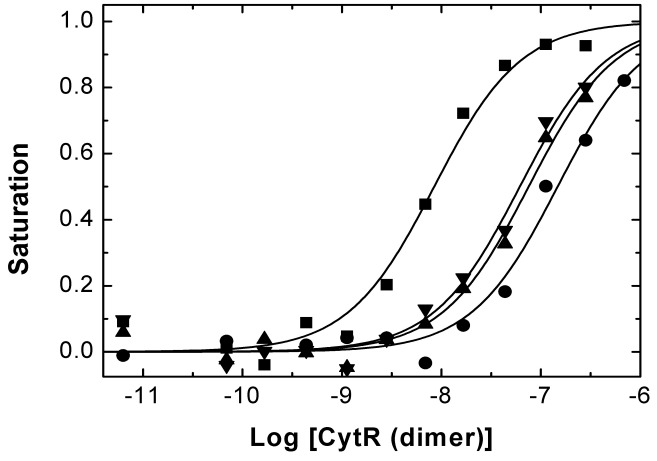

CytR binding to *nupGP* showing separate analysis of four distinct protected sites. Fractional saturation of CytO (■), CRP1 (▲), CRP2 (▼) and the proximal site (●) near the transcription start site are plotted as a function of log CytR dimer concentration. Solid curves represent the individual analysis of the protection data for each site according to Equation 1; these yield apparent individual site loading free energy changes equal to -10.8 ± 0.30 kcal/mol (CytO), -9.6 ± 0.35 kcal/mol (CRP1), -9.7 ± 0.40 kcal/mol (CRP2), -9.2 ± 0.35 kcal/mol (proximal CytR site).

site, similar to our previous observation for *cddP* (*5*). A partial match to the consensus CytR recognition motif that might account for this binding is indicated in Figure 1. Binding to the proximal site is weak in both protection and affinity, yielding $\Delta G_{prox} = -9.2 \pm 0.35$ kcal/mol. We also find the same affinity for CytR binding to CytO in wild type, CRP1$^-$ and CRP2$^-$ promoters, as expected. Table S1 has the complete results for CytR binding to *nupGP*.

Analysis of CytR binding to *tsxP2* proved more challenging. Footprint titrations of wild type *tsxP2* by CytR (Figure S4; lanes 1-12) show two distinct protected regions. That towards the top

Figure S4

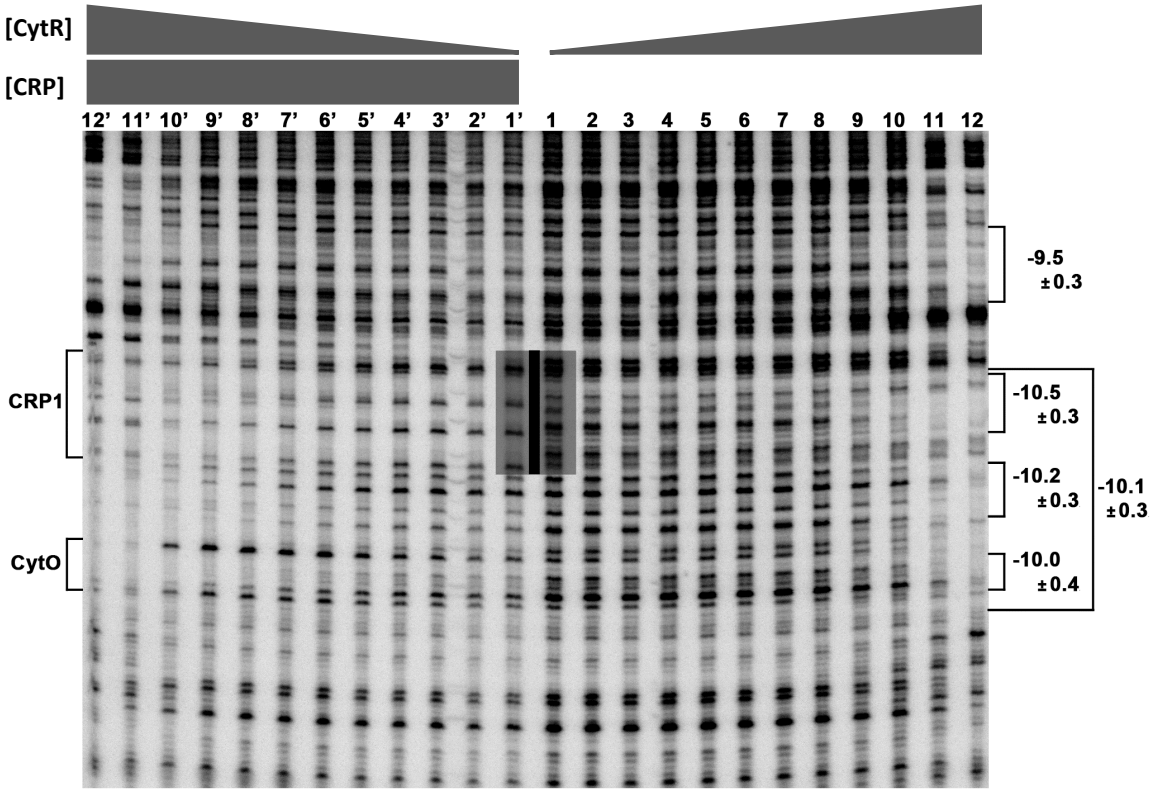

DNase I footprints of *tsxP2* as a function of [CytR]. *Lanes 1-12*, protection by CytR alone; *lanes 1'-12'*, protection by CytR in the presence of CRP; *Lanes 1 & 1'*, cleavage pattern in the absence of CytR. Solid bar and shaded region highlight the difference in cleavage pattern from CRP alone. CRP1 and of CytO are marked to the left of *lane 12'*. CytR binding results in a two distinct protected regions: a compact region near the top corresponding to the proximal site near the transcription start site, and an extended protected region that encompasses both CRP1 and CytO. Results from analysis of these regions to obtain apparent binding free energy changes are indicated to the right of *Lane 1*. Partitioning of the extended protected region yielded a slight gradient in apparent affinity, but did not distinguish separate sites.

represents a promoter proximal site for which we obtain $\Delta G_{prox} = -9.5 \pm 0.30$ kcal/mol. Below this is an uninterrupted region of protection that encompasses both CytO and CRP1, similar to an earlier report (*9*). The extent of the protected region suggests binding by more than one CytR dimer. However, we were unable to distinguish distinct binding sites from the protection data for CytR binding alone. Results from analyzing the entire extended protected region and of three smaller blocks included therein are indicated in Figure S4. The slight apparent gradation in affinity from promoter proximal to promoter distal within this region is not significant at the 95% level. Analysis of individual bands across the region yielded similar results. However, individual band analysis did distinguish two sites corresponding to CytO and CRP1 when CytR binding was analyzed in the presence of CRP as discussed just below.

3. Analysis of Cooperative and Competitive Binding of CRP and CytR

To evaluate cooperativity, the thermodynamic cycle for simultaneous binding of both proteins was analyzed as described previously (*5*). Binding of each protein (CytR and CRP) to wild type and reduced-valence promoters was investigated in the presence of a constant and near saturating concentration of the other protein. Figure S4 illustrates this strategy. Lanes 1-12 show CytR binding alone to *tsxP2*; lanes 1'-12' show CytR binding in the presence of CRP. CRP1 is indicated by the vertical bar between lanes 1 and 1'. The shaded area highlights differences in DNase I cleavage between unliganded (lane 1) and CRP-bound (lane 1'). These differences include both protected and hypersensitive bands.

Figure S5 shows the analysis of these CytR footprints in the absence (Figure S5A) and presence (Figure S5B) of CRP. Figure S5B shows the analysis of individual bands in lanes 1'-12' grouped according to their location in either CRP1 or in CytO. The behaviors of these two groups are quite distinct, thereby justifying the delineation CRP1 versus CytO protection as

Figure S5

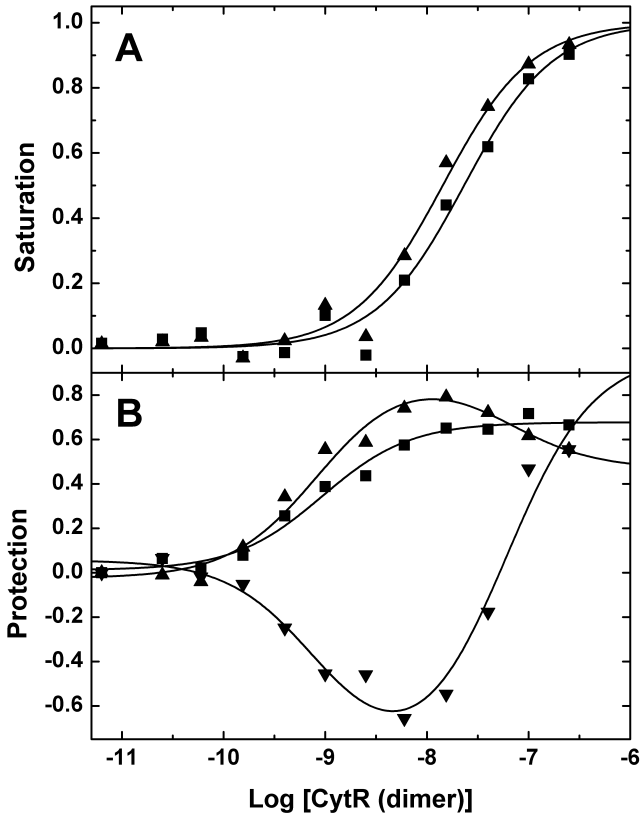

CytR binding to *tsxP2* from analysis of the DNase I footprint shown in Figure 5. The points represent analysis of binding to CytO (▲) and to a satellite CytR site located at CRP1 (■). These are distinguished as distinct CytR binding sites by different patterns of protection and hypersensitivity upon CytR binding in the presence of 0.1 μM CRP dimer as described in the text, i.e., biphasic for CytO versus monophasic for CRP1 *A*. Binding of CytR in absence of CRP. Analysis according to Equation 1 results in the solid lines; these yield apparent individual site loading free energy changes equal to-10.1 ± 0.37 kcal/mol (CytO) and -10.5 ± 0.27 kcal/mol (CRP1). *B*. Binding of CytR in presence of CRP. Individual bands were analyzed in the region corresponding to CytO. These were grouped and summed depending on whether first protected at lower CytR concentration and then hypersensitive at higher concentrations (▲), or the reverse (▼), yielding the two curves plotted. Analysis of the protection in CRP1 (■) yields an apparent individual site loading free energy change equal to -12.3 ± 0.22 kcal/mol. Global analysis of the two curves for CytO yields apparent individual site loading free energy changes equal to -12.2 ± 0.39 kcal/mol and -9.7 ± 0.45 kcal/mol for the first and second phases, respectively.

indicated by the brackets to the left of lane 12'. Bands located in CRP1 exhibit monotonic increasing protection as a function of CytR concentration (solid squares in Figure S5B). Analysis of this protection yields $\Delta G_{load,3} = -12.3 \pm 0.22$ kcal/mol. However, bands that are located in CytO are biphasic, thus indicating two binding events. These are either initially hypersensitive but subsequently becoming less so at higher concentrations of CytR, or initially

protected but subsequently becoming hypersensitive at higher concentrations of CytR. When the individual bands exhibiting each of these two behaviors are separately summed (solid triangles in Figure 6B) and analyzed globally according to a model that proposes two binding events, $\Delta G_{load} = -12.2 \pm 0.39$ and $\Delta G_{load} = -9.7 \pm 0.45$ kcal/mol are obtained. These necessarily represent distinct interactions between CytR and *tsxP2*, one of which cannot be due to local binding to CytO. Similarly, the protection in CRP1, which reflects only the higher affinity interaction, need not reflect local binding of CytR to CRP1. Indeed it seems most likely that this reflects an affect on DNase I accessibility resulting from binding of CytR to CytO to form a cooperative CytR-CRP complex.

Analysis of CytR binding alone, lanes 1-12, in the same manner supports this interpretation. With CytO and CRP1 defined by the same bands as analyzed in Figure S5B, the results shown in Figure 6A are obtained. Analysis of these data yields intrinsic free energy changes of $\Delta G_4 = -10.5 \pm 0.27$ kcal/mol (CRP1) and $\Delta G_3 = -10.1 \pm 0.37$ kcal/mol (CytO). Comparing the results obtained in the presence of CRP to these leads to the conclusion that the high affinity phase represents CytR binding to CytO, with higher affinity than CytR alone due to CytR-CRP cooperativity, while the lower affinity phase represents CytR binding to the CRP1 site, with lower affinity than CytR alone as a result of having to displace CRP. Table 2 has the complete results for CytR binding to *tsxP2*.

Similar experiments were conducted for wild type *nupGP* and for CRP1- & CRP2-promoters. Again, the binding curves in these cases reflect not just intrinsic binding to the local sites but also the effects of both cooperativity with interacting sites and competition between CytR and CRP for binding to overlapping sites at CRP1 and CRP2. Results are summarized in Table S1.

4. Effect of Cytidine

As noted above, cytidine binding to CytR is coupled to CytR-CRP cooperativity rather than to CytR-DNA binding as in other LacR family proteins. Given quite variable effects of cytidine binding on the individual pairwise interactions, as we have cataloged for other CytR-regulated promoters, it is of considerable interest to assess these effects at *nupGP*. The analysis of cooperativity described in the previous section was repeated in presence of 2 mM cytidine. Control experiments confirmed that cytidine binding has no affect on intrinsic DNA binding as in all previous cases. ΔG_{load} values obtained from these experiments are listed in Table S1.

5. Global Analysis

To delineate the effects of intrinsic binding, cooperativity and competition on the assembly of CytR-CRP regulatory complexes at these promoters, the fractional protection data for all of the titration experiments that contributed either to Table S1 for *nupGP* or to Table S2 for *tsxP2* were analyzed globally according to the molecular model defined by the promoter configurations in Table 3. This model is well-established from our previous analyses of *deoP2* (*6*), *udpP* (*3*) and *cddP* (*5*) and its major features are supported independently by results reported above. In consideration of the weak binding to CRP2 of tsxP2 we chose not to include this site in the analysis, opting instead to treat wild type *tsxP2* as $CRP2^-$.

The list of configurations accounts for CRP binding to CRP1 and to CRP2, and for CytR binding to CytO with both pairwise and three-way cooperativity between CytO and the CRP sites. It also accounts for CytR binding to the additional sites that occlude either CRP1 or CRP2. The model does not consider the promoter proximal CytR sites. Since there is no competition for CRP binding, CytR binding to this site is fully accounted by the ΔG_{load} for this site alone. The model has eight global parameters, consisting of free energy changes for intrinsic binding of

CytR to three sites, and of CRP to two sites (ΔG_i) and three cooperative free energy changes ($\Delta G_{ij(k)}$).

The fitting function for each individual-site titration is the sum of individual probabilities (eq. 2) for all configurations (Table 3) with the titrating protein bound to the site. Reduced-valence, $CRP1^-$ and $CRP2^-$ mutants are treated by excluding the configurations with protein bound to the mutated site. The protection endpoints constitute additional parameters that are local to each of the individual site binding curves. Normalized weights were applied as described (*Experimental Procedures*).

In analyzing *nupGP*, it is necessary to account for CRP binding to the mutated site CRP2 due to its high residual affinity. We defined $\Delta G_2'$ to account for this intrinsic binding and assumed the same cooperative interactions, ΔG_{23} and ΔG_{123}, as for the wild type site. $\Delta G_2'$ constitutes a ninth global fit parameter, one more than could be separately resolved from these data. The result when all parameters were allowed to float was an estimate for the intrinsic free energy of CytR binding to CytO, $\Delta G_3 = -11.4$ kcal/mol, that is poorly bounded and is inconsistent with the separate analysis of this parameter ($\Delta G_{load,3} = -10.4 \pm 0.3$ kcal/mol; Table S1) from simple titrations of CytR binding alone as in Figure 4. Consequently, we chose to fix $\Delta G_3 \equiv -10.4$ kcal/mol to estimate the remaining parameters. To account for effects of cytidine the cooperative interactions between CRP and cytidine-liganded CytR were denoted by $\Delta G_{ij(k)}(cyt)$. Analysis of data from forty-two separate titration experiments resulted in an excellent fit and well-bounded estimates of the free energy changes for all of the interactions in *nupGP* (Table S3).

Table S3: Global analysis of *nupGP* individual site binding data represented in Tables S1 and S2

Parameter	*nupG*[a]	*tsxP2*[a]
ΔG_1	-11.2 ± 0.1	-12.0 ± 0.4
ΔG_2	-14.1 ± 0.1	
$\Delta G'_2$	-12.6 ± 0.4	
ΔG_3	-10.4	-10.7 (+0.2, -0.3)
ΔG_4	-9.4 ± 0.1	
ΔG_5	-9.7 ± 0.1	
ΔG_{13}	-1.8 ± 0.1	-0.9 (+0.5, -0.2)
ΔG_{23}	-1.5 ± 0.1	
ΔG_{123}	-2.3 ± 0.1	
ΔG_{13}(cyt)	-1.1 ± 0.1	
ΔG_{23}(cyt)	-1.0 ± 0.1	
ΔG_{123}(cyt)	-1.3 ± 0.1	
s[b]	0.013	0.054

[a] ΔG's in kcal/mol ± the 65% confidence interval. Asymmetric confidence limits are noted separately in parenthesis where applicable.

[b] Square root of the variance of the fitted curves.

Analysis of *tsxP2* treated the wild type promoter as CRP2$^-$, that is assumed no specific binding of CRP to CRP2 rather than accounting explicitly for the very weak affinity. In fact, if this affinity is as high as the upper limit we were able to determine (Table 2) CRP2 could be up to 50% occupied 0.1 μM CRP. While ignoring this binding will affect the quality of the fit it should not affect the parameter values, and in particular ΔG_{13}, appreciably. Results from this global analysis of the *tsxP2* binding data are reported in Table S3.

References

1. Pedersen, H., Dall, J., Dandanell, G., and Valentin-Hansen, P. (1995) Gene-regulatory modules in Escherichia coli: nucleoprotein complexes formed by cAMP-CRP and CytR at the nupG promoter, *Mol Microbiol 17*, 843-853.

2. Ackers, G. K., Shea, M. A., and Smith, F. R. (1983) Free energy coupling within macromolecules. The chemical work of ligand binding at the individual sites in co-operative systems, *J Mol Biol 170*, 223-242.

3. Gavigan, S. A., Nguyen, T., Nguyen, N., and Senear, D. F. (1999) Role of multiple CytR binding sites on cooperativity, competition, and induction at the Escherichia coli udp promoter, *J Biol Chem 274*, 16010-16019.

4. Holst, B., Sogaard-Andersen, L., Pedersen, H., and Valentin-Hansen, P. (1992) The cAMP-CRP/CytR nucleoprotein complex in Escherichia coli: two pairs of closely linked binding sites for the cAMP-CRP activator complex are involved in combinatorial regulation of the cdd promoter, *Embo J 11*, 3635-3643.

5. Holt, A. K., and Senear, D. F. (2010) An unusual pattern of CytR and CRP binding energetics at Escherichia coli cddP suggests a unique blend of class I and class II mediated activation, *Biochemistry 49*, 432-442.

6. Perini, L. T., Doherty, E. A., Werner, E., and Senear, D. F. (1996) Multiple specific CytR binding sites at the Escherichia coli deoP2 promoter mediate both cooperative and competitive interactions between CytR and cAMP receptor protein, *J Biol Chem 271*, 33242-33255.

7. Sogaard-Andersen, L., Mollegaard, N. E., Douthwaite, S. R., and Valentin-Hansen, P. (1990) Tandem DNA-bound cAMP-CRP complexes are required for transcriptional repression of the deoP2 promoter by the CytR repressor in Escherichia coli, *Mol Microbiol 4*, 1595-1601.

8. Das, R., Laederach, A., Pearlman, S. M., Herschlag, D., and Altman, R. B. (2005) SAFA: Semi-automated footprinting analysis software for high-throughput quantification of nucleic acid footprinting experiments, *Rna 11*, 344-354.

9. Gerlach, P., Sogaard-Andersen, L., Pedersen, H., Martinussen, J., Valentin-Hansen, P., and Bremer, E. (1991) The cyclic AMP (cAMP)-cAMP receptor protein complex functions both as an activator and as a corepressor at the tsx-p2 promoter of Escherichia coli K-12, *J Bacteriol 173*, 5419-5430.